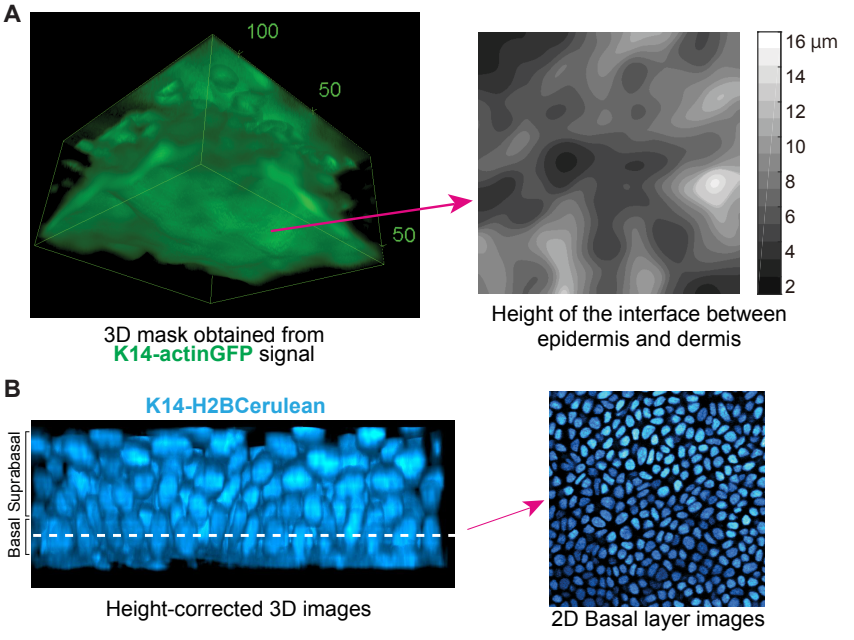
A
100
50
50
16 µm
14
12
10
8
6
4
2
3D mask obtained from
K14-actinGFP signal
Height of the interface between
epidermis and dermis
B
K14-H2BCerulean
Basal
Suprabasal
Height-corrected 3D images
2D Basal layer images

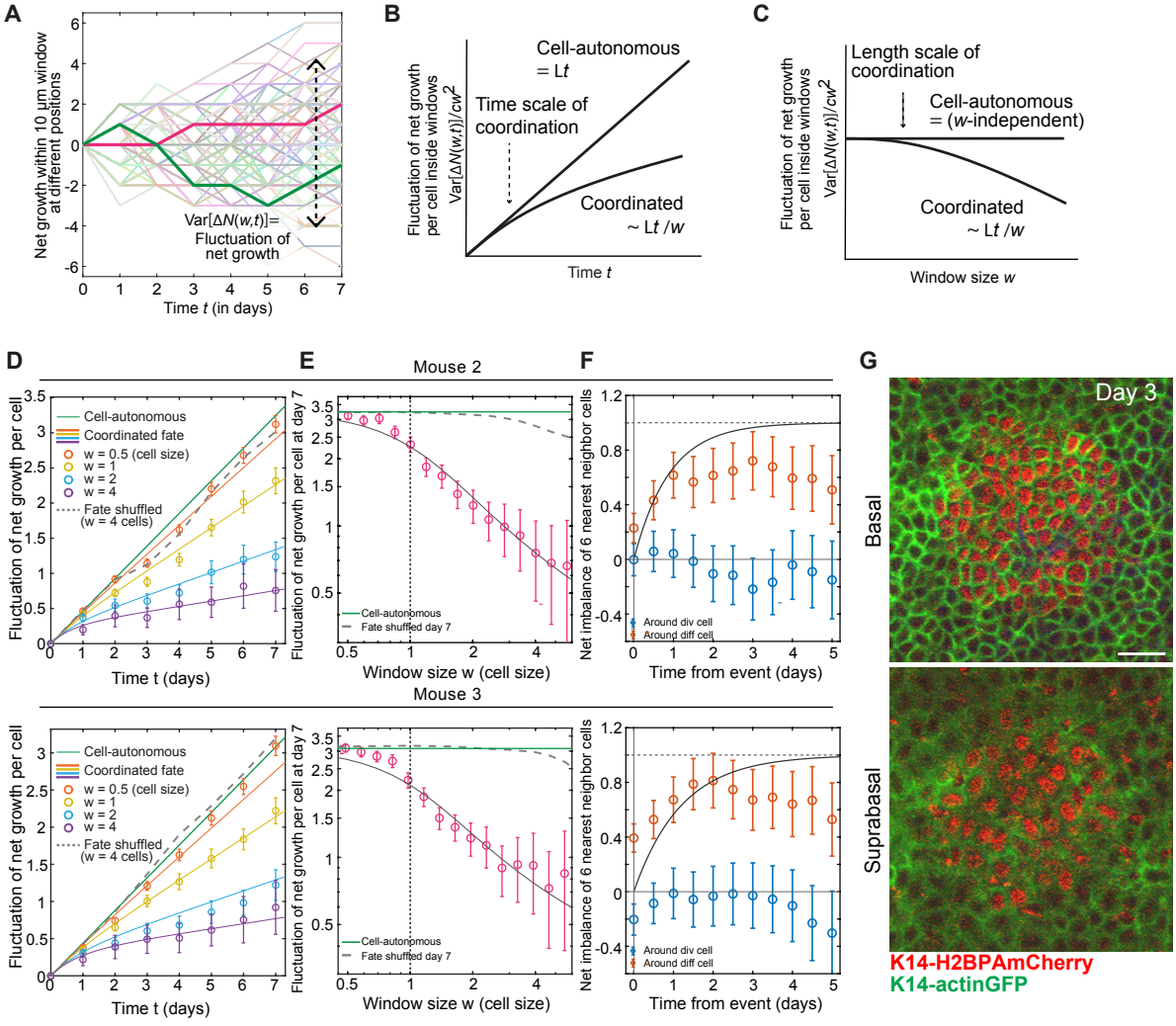
A
Net growth within 10 μm window at different positions
Var[ΔN(w,t)]= Fluctuation of net growth
Time t (in days)
B
Fluctuation of net growth per cell inside windows Var[ΔN(w,t)]/cw2
Cell-autonomous = Lt
Time scale of coordination
Coordinated ~ Lt /w
Time t
C
Fluctuation of net growth per cell inside windows Var[ΔN(w,t)]/cw2
Length scale of coordination
Cell-autonomous = (w-independent)
Coordinated ~ Lt /w
Window size w
D
Mouse 2
Fluctuation of net growth per cell
Cell-autonomous
Coordinated fate
w = 0.5 (cell size)
w = 1
w = 2
w = 4
Fate shuffled (w = 4 cells)
Time t (days)
E
Fluctuation of net growth per cell at day 7
Cell-autonomous
Fate shuffled day 7
Window size w (cell size)
F
Net imbalance of 6 nearest neighbor cells
Around div cell
Around diff cell
Time from event (days)
Mouse 3
G
Day 3
Basal
Suprabasal
K14-H2BPAmCherry
K14-actinGFP

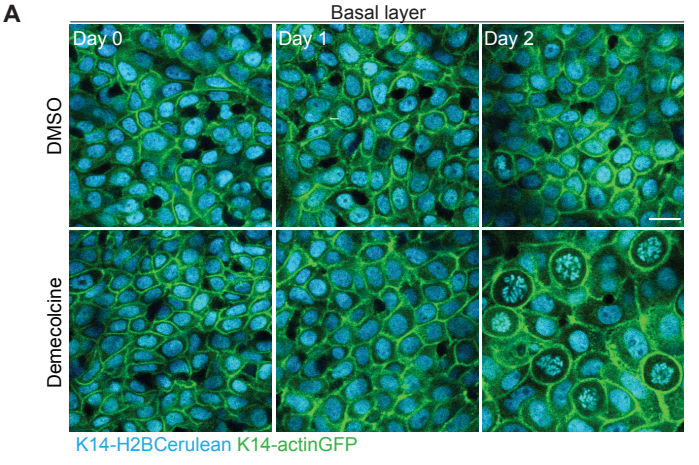
A
Basal layer
Day 0
Day 1
Day 2
DMSO
Demecolcine
K14-H2BCerulean K14-actinGFP

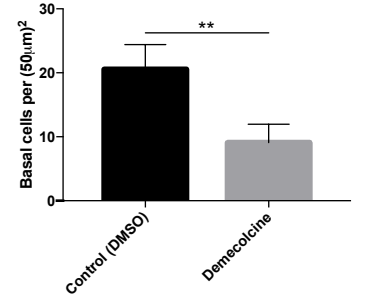
B
Basal cells per (50μm)²
30
20
10
0
**
Control (DMSO)
Demecolcine

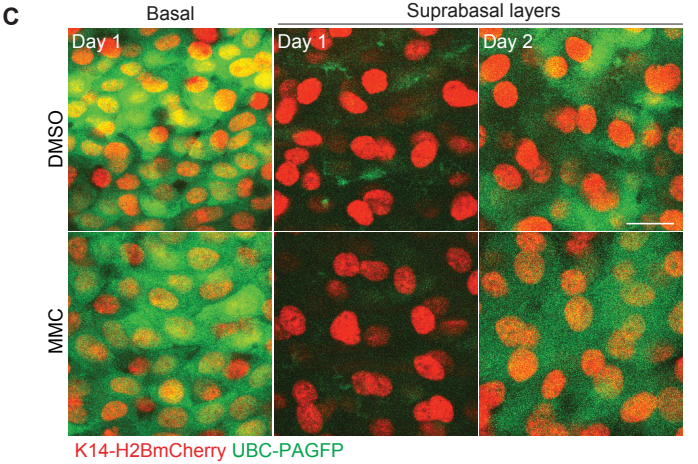
C
Basal
Suprabasal layers
Day 1
Day 1
Day 2
DMSO
MMC
K14-H2BmCherry UBC-PAGFP

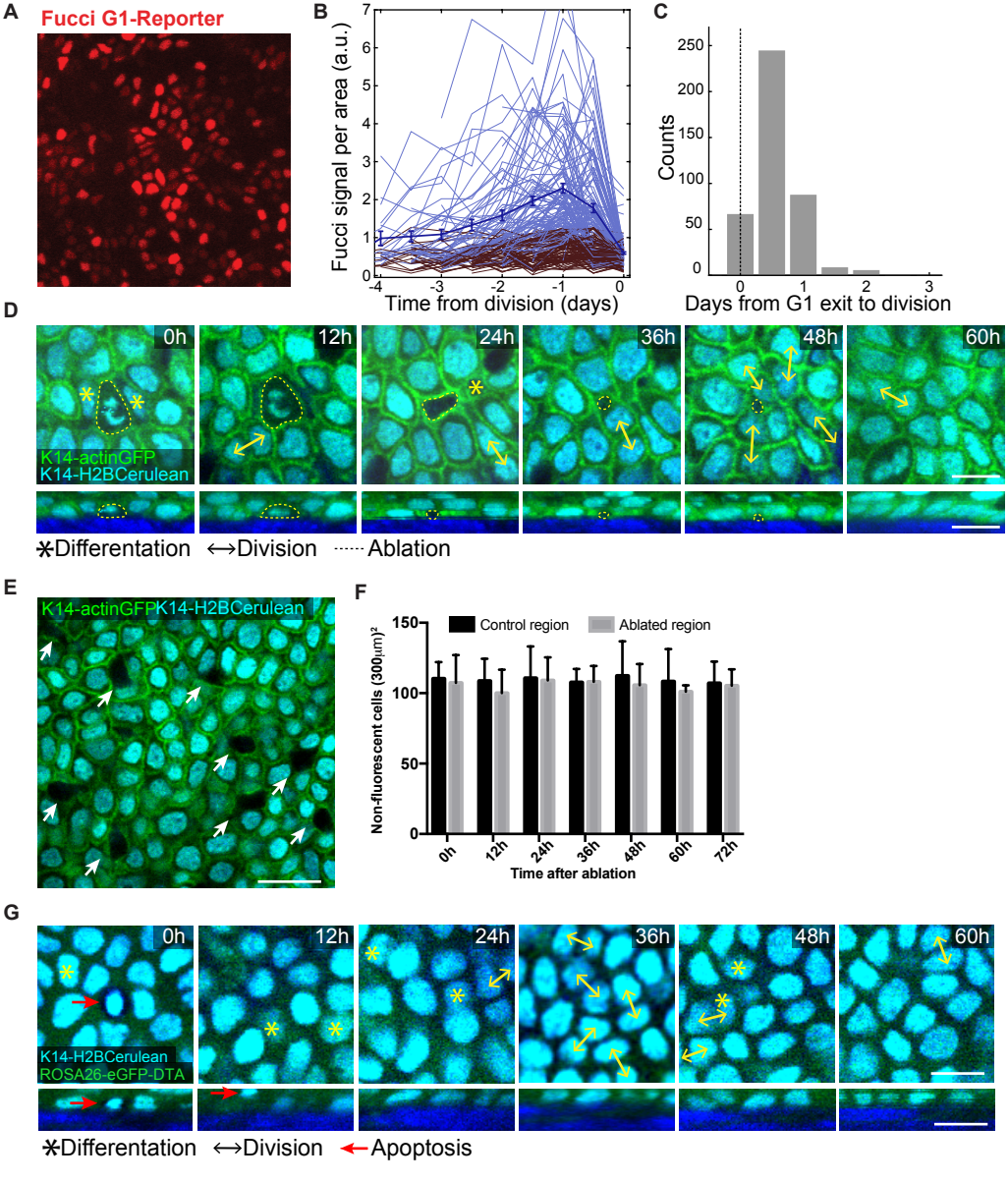
A
Fucci G1-Reporter
B
Fucci signal per area (a.u.)
Time from division (days)
C
Counts
Days from G1 exit to division
D
0h
12h
24h
36h
48h
60h
K14-actinGFP
K14-H2BCerulean
Differentation
Division
Ablation
E
K14-actinGFPK14-H2BCerulean
F
Control region
Ablated region
Non-fluorescent cells (300μm)²
Time after ablation
G
K14-H2BCerulean
ROSA26-eGFP-DTA
Differentation
Division
Apoptosis

Supplemental Information:

Figure S1. Schematic of image analysis, Related to Figure 1
(A) Left: example of a 3D structure of the epidermis reconstructed from *the K14-actinGFP* signal. Raw z-stack image was Gaussian blurred to represent an intact structure. Right: height of the interface between the epidermis (*K14-actinGFP* positive) and dermis (*K14-actinGFP* negative) for the left example 3D structure.
(B) Left: original *K14-H2BCerulean* image after height correction using information of (A). Right: by selecting a z-plane close to the bottom in the height-corrected data, we obtain a 2D image of the basal layer in all channels.

Figure S2. Replicate of fluctuation and neighbor imbalance analyses in mouse 2 and mouse 3, and details of circular labeling experiment, Related to Figures 2 and 3
(A) Time course of net growth within a window height/width of 10 μm (1.4 cell size) at 500 different randomly picked positions. Green and magenta lines are typical examples of the time course.
(B) Cell-autonomous and coordinated fate models predict different behaviors in the time evolution of net growth fluctuation.
(C) Cell-autonomous and coordinated fate models predict different behaviors in the window size dependence of net growth fluctuation.
(D) Fluctuation of net growth as a function of time in mouse 2 and mouse 3
(E) Fluctuation of net growth as a function of window size. Mouse 2: n = 354 divisions and 330 differentiations. Mouse 3: 299 divisions and 316 differentiations. Both within 90 μm x 90 μm areas of the basal layer in 7 days. Fitted parameters: τ = 0.9 day, l = 5.2 μm for mouse 2, τ = 1.2 days, l = 5.0 μm for mouse 3.
(F) Neighbor net imbalance analysis conducted for Mouse 2 (363 differentiations and 334 divisions) and Mouse 3 (307 differentiations and 324 divisions). Solid lines: $1 - e^{-t/\tau}$, where τ = 0.9 day for Mouse 2, τ = 1.2 days for Mouse 3.
(G) Basal layer cells inside circles with radius of 50 μm were labeled with *K14H2B-PAmCherry* and followed for three days in the basal and suprabasal layers.

Figure S3. Blocking stem cell division, Related to Figure 4
(A) Representative images of basal cell density during Demecolcine induced cell division block in mouse ear. Scale bar indicates 10 μm.
(B) Quantification of basal cell density after 2 days of Demecoline treatment in the mouse ear. (n = 15 regions from three mice; error bars represent s.d.)
(C) Representative images of *UBC-PAGFP* labeled cells traced after Mitomycin C (MMC) treatment. Differentiation of labeled cells into suprabasal layers appears unaffected by MMC treatment. Scale bar indicates 10 μm. See also quantification in Figure 4E.

Figure S4. Fucci G1 reporter analysis and laser ablation assay, Related to Figures 5 and 6

(A) Representative image of the Fucci-G1 reporter (*mKO2-hCdt1(30/120)*) in the basal layer, showing variable levels of fluorescence between individual cells.
(B) Fucci-G1 reporter signal per nuclear area as a function of time from division in one of the regions from mouse 1. Endpoint of time ($t = 0$) is taken as the cell division time. Blue: G1-reporter positive cells. Dark red: G1-reporter negative cells. Dark blue solid line corresponds to the average of the signal/area for the G1-reporter positive population. Discrimination between G1 signal positive ($s_f(i) = 1$, 120 traces) and negative ($s_f(i) = 0$, 143 traces) was based on a threshold in the maximum value of signal/area. See STAR Methods for detail.
(C) Histogram of time elapsed between G1 exit, as indicated by Fucci-G1 signal, and basal cell division. Note the predictable time window between G1 exit and division (4 regions from 3 mice, n = 411 dividing cells).
(D) Closely spaced revisits after targeted ablation of a single epidermal basal cell. Between 12 and 24 hours post ablation, the targeted cell loses its nuclear signal and shrinks its size significantly (indicated by the dotted yellow line). By 36 hours the cell is effectively eliminated from the tissue. Scale bar indicates 10 μm.
(E) Representative image of non-epithelial marker positive (likely immune) cells in the epidermis of a *K14actin-GFP; K14-H2BCerulean* mouse.
(F) Quantification of non-epithelial marker positive cells, showing no significant difference between control regions and those containing ablated cells (6 fields of view containing 10-15 ablated cells per field from 3 mice).
(G) Closely spaced revisits after DTA induction in low numbers of basal cells. By 24 hours after Tamoxifen injection (designated as 0h), individual cells (marked by the red arrow) lose their cytoplasmic eGFP signal, indicating that recombination has occurred and DTA is being expressed, and display a compacted and/or fragmented nucleus. Over the next 12-24 hours, the dying cell moves upward and is eliminated from the basal layer. Scale bar indicates 10 μm.

Movie S1. Live image sequence of nuclei in the mouse epidermis basal layer, Related to Figure 1
Left: optical section of basal layer cells (*K14-H2BCerulean*) in a region of size 90 μm x 90 μm. Right: result of whole cell population tracking. Colors represent clones from the initial timepoint, and the regions of colors represent the voronoi diagram calculated from the position of the cells (local maxima in *K14-H2BCerulean* signal intensity). 1 frame = 12 hours.

Movie S2. Live image sequence of cell cortex in the mouse epidermis basal layer, Related to Figure 5
Left: optical section of basal layer cells (*K14-ActinGFP* signal with *K14-H2BCerulean* signal values subtracted, see STAR Methods for detail) in the same region as Movie S1. Right: result of whole cell population tracking. Colors represent clones from the initial timepoint, and the regions of colors are the result of marker-controlled watershed segmentation. 1 frame = 12 hours.

Movie S3. Live image sequence of Fucci-G1 marker in the mouse epidermis basal

layer, Related to Figure 5
Left: optical section of basal layer cells (Fucci-G1 marker) in the same region as Movie S1. Right: segmentation based on cell cortex signal (same as Movie S2). 1 frame = 12 hours.

Movie S4. Live image sequence of CAG::H2B-GFP cells after small and large laser ablations, Related to Figure 6.
Left: large field of view from a *CAG::H2B-GFP* mouse showing 9 basal cells recently targeted with sub-micron scale laser ablation (red arrows). The ubiquitous H2B-GFP expression in these mice allows us to look in an unbiased manner for any signs of immune cell infiltration following ablation.
Right (top): close-up of epithelial region surrounding one ablated basal cell (red outline and arrow), showing no signs of recruitment from non-epithelial cells.
Right (middle): close up of dermal region underlying the same ablated cell as in the top panel, showing no recruitment of cells from the dermis.
Right (bottom): close up of a dermal region after a much larger laser ablation (~20 μm x 30 μm; red outline). In this case, *CAG::H2B-GFP* expression allows us to visualize recruitment of large numbers of cells in the hours following damage. Scale bars in all panels indicate 20 μm. 1 time frame = 5 minutes.

Methods S1: Statistical corrections and fitting formulas, related to STAR Methods

Note 1. Statistical correction for overlapping random samples

Randomly positioning windows with size w in a finite image region of size L will lead to overlaps. The overlap affects the number of independent windows that contribute to $\Delta N(w,t)$, and will effectively decrease the fluctuation. When randomly putting two windows inside a region of $(2w \le L)$, the expected proportion of overlap in the area is

$$O(L,w) = \frac{w^2}{(L-w)^2}\left(1-\frac{w}{3(L-w)}\right)^2. \quad (1)$$

We divided the variances calculated as described in STAR Methods by $1-O(L,w)$.

Equation (1) is derived as follows. Randomly placing a line segment with length w to fit inside the region with length $L(\ge w)$ is equivalent to randomly sampling the left edge of the segment from $[0, L-w]$. Taking two random positions x_1 and x_2 from $[0, L-w]$, the probability distribution of the distance between x_1 and x_2, $\Delta_x = |x_1 - x_2|$, is $P(\Delta_x) = (L - w - \Delta_x)/(L-w)^2$ for $0 \le \Delta_x \le L-w$ and zero otherwise. The overlapping fraction of the two segments with the left edges positioned at x_1 and x_2 is $1-\Delta_x/\mathrm{w}$ for $0 \le \Delta_x \le w$ and zero otherwise. We next introduce a second direction y to randomly place line segments with bottom edges placed at y_1 and y_2. We then have two windows with the bottom left corners with the coordinates (x_1, y_1) and (x_2, y_2). Assuming that $L - w \ge w$ $(2w \le L)$, the average overlapping fraction of the two windows is then

$$\begin{aligned} O(L,w) &= \int_0^w d\Delta_x \int_0^w d\Delta_y P(\Delta_x)P(\Delta_y)\left(1-\frac{\Delta_x}{w}\right)\left(1-\frac{\Delta_y}{w}\right) \\ &= \frac{w^2}{(L-w)^2}\left(1-\frac{w}{3(L-w)}\right)^2. \quad (2) \end{aligned}$$

Note 2. Length- and time-scales of fate imbalance in a generalized model of fate coordination

Here we describe the generalized stochastic model used in the fittings presented in Figures 2B, 2C, S2D and S2E. We assume that the fate choice events, differentiation or division, will all happen in a coordinated manner but with stochastic time difference $s > 0$ and *xy*-displacement (ξ, η). We assume for simplicity that s is sampled from an exponential distribution: $P(s) = e^{-s/\tau}/\tau$, and (ξ, η) is sampled from a Gaussian distribution: $P(\xi,\eta) = e^{-(\xi^2+\eta^2)/2l^2} / 2\pi l^2$. Here, τ and l are the time scale and length scale of the coordination, respectively, which are the fitting parameters. We also assume that s and (ξ, η) are independent from each other. This simple model is used to fit the key features of the data and to gain an intuition for the effect of lags and coordination distance on the observed behaviors, and is not intended to reflect any specific mechanism of fate coupling.

We consider a three-dimensional box with width and height of the window size w and the depth of the time length t. Sampling the pairs of events randomly across space and

time, and assigning the above probability for the time difference and the displacement between the fate-coordinated pairs, we count the divisions that happened inside this box as +1 and the differentiations as -1, corresponding to cell increase and decrease events, respectively. We are interested in the statistics of the net growth, $\Delta N(w,t)$, which is the sum of the +1 and -1's that occurred inside the box.

Since the contributions from the fate-coordinated events are zero (one differentiation and one division amounts to ± 0), and since the isolated events (events inside the box that have a fate-coordinated pair outside the box) are binomially distributed between division (+1) and differentiation (-1) fates, the variance of $\Delta N(w,t)$ is equal to the average number of isolated events. Given that one of the events is sitting inside the box, the probability of the fate-coordinated event to be also sitting inside the box is

$$Q_{\tau l}(w,t) = Q_\tau(t)\, Q_l(w), \qquad (3)$$

where $Q_\tau(t)$ is the probability of finding the fate-coordinated event inside the time frame t, and $Q_l(w)$ is the probability of finding the fate-coordinated event inside the window of size w.

The average number of total events inside the box is $\Lambda w^2 t$, where $\Lambda = c\,(\lambda + \Gamma)$ is the rate per area of events with λ, Γ, and c being the steady-state cell division rate, differentiation rate, and cell density. The average number of isolated events, and thus the variance of $\Delta N(w,t)$, is obtained as

$$\mathrm{Var}[\Delta N(w,t)] = \Lambda w^2 t \frac{1 - Q_{\tau l}(w,t)}{1 + Q_{\tau l}(w,t)}. \qquad (4)$$

Here, the factor arises from the ratio of the isolated vs coordinated cells in the total of events, $1 - Q_{\tau l}(w,t) : 2Q_{\tau l}(w,t)$. The factor 2 here arises from the pairs of cells that are both inside the box contributing as 2 cells in the total number.

We first compute $Q_\tau(t)$. Assuming that the time difference between the two events is s, the probability of finding both events within the time frame t under the condition that at least one is inside, is $1 - s/t$. Taking the average of this probability over s, we have

$$Q_\tau(t) = \int_0^t ds\, P(s)\left(1 - \frac{s}{t}\right) = 1 - \frac{\tau}{t}\left(1 - e^{-\frac{t}{\tau}}\right). \qquad (5)$$

Note that the integral is only taken up to *t* since for pairs of events which are further apart from t, there is no possibility of finding both events inside the interval t.

Similarly, by assuming that the *xy* displacement between the two events is (ξ, η), the probability of finding both events fitting inside the window of size *w* under the condition that at least one is inside, is $(1 - |\xi|/w)(1 - |\eta|/w)$. Taking the average of this probability over (ξ, η), we have

$$\begin{aligned} Q_l(w) &= \int_{-w}^{w} d\xi \int_{-w}^{w} d\eta\, P(\xi,\eta)\left(1 - \frac{|\xi|}{w}\right)\left(1 - \frac{|\eta|}{w}\right) \\ &= \left[\mathrm{Erf}\left(\frac{w}{\sqrt{2}l}\right) + \sqrt{\frac{2}{\pi}}\frac{l}{w}\left(e^{-\frac{w^2}{2l^2}} - 1\right)\right]^2. \qquad (6) \end{aligned}$$

Here, $\mathrm{Erf(x)} = \frac{2}{\sqrt{\pi}}\int_0^x dt e^{-t^2}$ is the error function.

Together, Eqs. (4) and (6) provide an exact formula for the expected shape of $\mathrm{Var}[\Delta N(w,t)]$, which is used in fitting for the lengthscale and timescale of fate coordination as described in STAR Methods.

To understand how the coordination in fate affects $\mathrm{Var}[\Delta N(w,t)]$, we consider two limiting cases: $l/w, \tau/t \to \infty$ and $l/w, \tau/t \to 0$. In the first case, since the fate-coordinated pairs are so far apart in time and space compared with t and w, the fluctuation should be equivalent to the case of the cell-autonomous model. Indeed, $Q_\tau(t), Q_l(w) \to 0$ in this limit, meaning that

$$\frac{\mathrm{Var}[\Delta N(w,t)]}{w^2} \simeq \Lambda t. \quad \left(\text{for } \frac{l}{w}, \frac{\tau}{t} \to \infty\right) \qquad (7)$$

which is the statistics of the cell-autonomous model. In the second case, since t and w are much bigger than the coordination time and length scales, the isolated events can only be found near the surface of the box, meaning that the fluctuation should be one order smaller than the cell autonomous case in terms of t or w. We obtain $Q_\tau(t) \simeq 1 - \tau/t$, and $Q_l(w) \simeq 1 - \sqrt{8/\pi}\, l/w$ in the lowest order of l/w and τ/t, which leads to

$$\frac{\mathrm{Var}[\Delta N(w,t)]}{w^2} \simeq \frac{1}{2}\Lambda\tau + \sqrt{\frac{2}{\pi}}\frac{\Lambda l}{w}t. \qquad \left(\text{for } \frac{l}{w}, \frac{\tau}{t} \to 0\right) \qquad (8)$$

Here, the first term is a constant that does not depend on t, which is the contribution from the isolated events close to the initial timepoint or the final timepoint. The second term is linear in time but inversely proportional to w, which is the contribution from the isolated events sitting close to the edge of the window.

Note 3. Background-detrending the net imbalance around differentiation and division events

For each cell, labeled by *i*, there is the birth time $t_b(i)$, the fate choice time $t_f(i)$, and the fate $\sigma(i)$. The fate $\sigma(i)$ is +1 for a dividing cell, and -1 for a differentiating cell. If the cell was present at the initial time point $t = 0$, we set $t_b(i) = -\infty$. If the fate was not chosen before $t_{\max}$, which is the last time point of the image sequence, we set $t_f(i) = \infty$ and $\sigma(i) = \mathrm{NaN}$. Let us define the time course of imbalance for $t_b(i) \le t < t_{\max}$:

$$I(i,t) = \begin{cases} 0 & \left(t \le t_f(i)\right) \\ \sigma(i) & \left(t > t_f(i)\right) \end{cases}. \qquad (9)$$

For *t* outside of this defined region, $I(i,t)$ returns NaN.

We denote the label of the *k*-th nearest neighbor of cell *i* (in terms of *xy*-coordinate) at time *t* as $NN(i,t,k)$. For each fate decision event of cell *i*, we calculated the net imbalance of the *K*-nearest neighbor cells in the subsequent time course:

$$I^{\mathrm{NN}}(i,t,K) = \sum_{k=1}^{K} I\big(NN\big(i, t_f(i), k\big), t_f(i) + t\big), \qquad (10)$$

where $t_f(i) \le t < t_{\max}$. Again, for t outside of this defined region, $I^{\mathrm{NN}}(i,t,K)$ returns NaN. The sum in the right-hand side skips entries with NaN values.

To obtain the background imbalance, we first define $N(t)$ as the number of cells that existed at time *t*, and $C(t,j)$ as the label of the *j*-th cell at time *t* $(1 \le j \le N(t))$. The background imbalance within the imaged region is calculated as

$$B(t_1, t_2) = \frac{1}{N(t_1)} \sum_{j=1}^{N(t_1)} I(C(t_1, j), t_2), \qquad (11)$$

for $t_1 < t_2$. Note that $B(t_1, t_2) \neq 0$ even in the ideal case (i.e., infinite number of samples and time constant rates). This is because the number of dividing cells vs differentiating cells within a randomly selected population is not 0.5 when the average lifetimes of dividing cells and differentiating cells are different.

By subtracting the background imbalance, we calculated the de-trended net imbalance around differentiation and division events as functions of the number of neighbors *K* and $t \geq 0$:

$$I^{\mathrm{diff}}(t, K) = \frac{1}{n_{\mathrm{f}}(t)} \sum_{i:\sigma(i)=-1} [I^{\mathrm{NN}}(i, t, K) - K \cdot B\big(t_f(i), t_f(i) + t\big)], \qquad (12)$$

$$I^{\mathrm{div}}(t, K) = \frac{1}{n_{\mathrm{v}}(t)} \sum_{i:\sigma(i)=+1} [I^{\mathrm{NN}}(i, t, K) - K \cdot B\big(t_f(i), t_f(i) + t\big)]. \qquad (13)$$

Here, $n_{\mathrm{f}}(t)$ and $n_{\mathrm{v}}(t)$ are the total number of differentiation and division events that have $I\left(i, t + t_f(i)\right) \neq \mathrm{NaN}$, respectively. The indices i of differentiating (dividing) cells is denoted as $i : \sigma(i) = -1\ (+1)$ for the sum. Again, the sum in the right-hand side skips entries with NaN values.

Note 4. Formulae for area growth

We denote the cell area (calculated from the Actin-GFP based segmentation) of cell i at time t as $A(i, t)$. If cell i did not exist at time t, then $A(i, t) = \mathrm{NaN}$. The time course of the average cell area for differentiating/dividing cells are ($t \leq 0$)

$$A^{\mathrm{diff}}(t) = \frac{1}{n_{\mathrm{f}}(t)} \sum_{i:\sigma(i)=-1} A(i, t_f(i) + t), \qquad (14)$$

$$A^{\mathrm{div}}(t) = \frac{1}{n_{\mathrm{v}}(t)} \sum_{i:\sigma(i)=+1} A\big(i, t_f(i) + t\big). \qquad (15)$$

The sum in the right-hand side skips entries with NaN values.

The time frame of largest cell area growth is,

$$t_{AG}(i) = \underset{t}{\mathrm{argmax}}\ [A(i, t + 12\ \mathrm{hours})/A(i, t)]. \qquad (16)$$

Note 5. Background-detrended past accumulated net imbalance:

For dividing cells i with positive G1-reporter signal, we obtained the timepoints of the largest cell area growth, $t_{AG}(i)$ (Equation (16)). For t within $t_b(i) < t_{AG}(i) + t \leq t_d(i)$, we computed the past accumulated imbalance:

$$I^{\mathrm{BNN}}(i, K, t) = \sum_{s=t_b(i)-t_{AG}(i)+1}^{t} \sum_{k=1}^{K} I(NN(i, t_{AG}(i) + s, k), t_{AG}(i) + s). \qquad (17)$$

The background of this quantity is the net growth per cell calculated between two time points:

$$B^{\mathrm{G}}(t_1, t_2) = \frac{N(t_2) - N(t_1)}{N(t_1)}\,. \qquad (18)$$

Note that in contrast to $B(t_1, t_2)$, the background $B^{G}(t_1, t_2)$ is zero in the ideal case where there are no fluctuations in division and differentiation rates, irrespective of cell lifetimes. By subtracting this background, we obtained the past accumulated net imbalance:

$$I^{\mathrm{B}}(t, K) = \frac{1}{n_{\mathrm{dv}}(t)} \sum_{i:\, s_f(i)=1} [I^{\mathrm{BNN}}(i, t, K) - K \cdot B^{\mathrm{G}}(t_b(i), t_{AG}(i) + t)]. \qquad (19)$$

Here, $n_{dv}(t)$ is the number of dividing cells that had positive G1-reporter signal and $I\big(i, t + t_d(i)\big) \neq \mathrm{NaN}$. The sum in the right-hand side skips entries with NaN values.